A dumbbell's random walk in continuous time

1994 J. Phys. A: Math. Gen. 27 7733

(http://iopscience.iop.org/0305-4470/27/23/016)

J. Phys. A: Math. Gen. 27 (1994) 7733–7738. Printed in the UK

A dumbbell's random walk in continuous time

P A Alemany†, R Vogel, I M Sokolov‡ and A Blumen

Theoretische Polymerphysik, Universität Freiburg, Rheinstraße 12, D-79104 Freiburg i.Br., Germany

Received 5 July 1994, in final form 6 September 1994

Abstract. We study the continuous-time dynamics of a rigid dumbbell or, equivalently, of two random walkers coupled through a holonomic constraint. Random walkers under holonomic constraints provide a generic model for many physical systems, e.g. for polymers. Interestingly, the spatial and temporal aspects of the dumbbell's motion are highly coupled: the ensuing behaviour differs considerably from a simple continuous-time random walk (CTRW)-picture. For waiting-time distributions with broad probability densities the dumbbell's dynamics parallels that of polymers in melts, in that two diffusive regimes appear, connected by a broad crossover region. We determine analytically the diffusion constants in the two regimes from a higher-order decoupling approach; the results agree well with simulations.

In the present work we study the motion of a rigid dumbbell, consisting of two beads connected by a segment. The dumbbell moves along a straight line by performing flips, see figure 1: The two beads move according to waiting-time distributions (WTD), familiar from continuous-time random walk (CTRW) models [1–4]. Due to the jumps, the *dumbbell's centre of mass (CM) makes a step to the left (to the right) when the right* (the left) bead jumps. The motion of the CM is thus a 1D random walk (RW), whose properties will be considered in the following.

This problem is of interest because the dumbbell represents the simplest model for a system of random walkers which move under mutual geometrical (holonomic) constraints. As we proceed to show, under such constraints and broad WTD the spatial and the temporal aspects of the CM's walk are strongly coupled. This may be contrasted with the simple CTRW-picture for independent particles, where usually the spatial and temporal aspects decouple [5].

The existence of holonomic constraints is a generic feature for many systems, polymers being an important example. Our study is thus motivated by a phenomenological approach to polymer diffusion in melts [6] and allows us to analyse aspects of the spatio-temporal coupling [7, 8] which arise in the CTRW-framework.

We recall that the motion of polymers in melts is complex: The CM's motion is diffusive at short and long times and shows a marked crossover in between, explained mostly by a change from Rouse to reptation dynamics [9–11]. Another description of this phenomenon starts from the Orwoll–Stockmayer polymer model [12, 13] of N

† Also at Centro Atómico Bariloche (CNEA) and Instituto Balseiro (UNC), 8400 Bariloche, Argentina.
‡ Also at P N Lebedev Physical Institute of the Academy of Sciences of Russia, Leninsky Prospekt 53, Moscow 117924, Russia.

0305-4470/94/237733+06$19.50

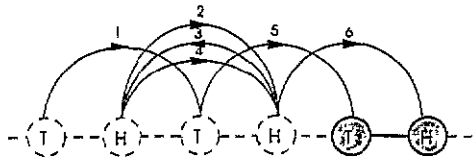

Figure 1. Six consecutive jumps of the dumbbell, whose end position is shown in grey. Note that the head (H) and the tail (T) move independently of each other.

beads, connected by $N-1$ freely jointed rods. The beads perform jumps according to specific rules (i.e. 180°-rotations of two neighbouring rods around the axis defined by the neighbouring beads; the end beads re-orient freely). One then lets the times at which the beads jump follow general WTD [6], the rationalization of the WTD being, for example, as suggested by Glarum [14], based on the 'free volume' picture: for any bead to move in the melt a vacancy is required. As examples, the waiting times may have probability densities (PD) of exponential type

$$\psi(t) = \tau^{-1} \exp(-t/\tau) \tag{1}$$

or of algebraic type

$$\psi(t) = \gamma/(1+t)^{1+\gamma}. \tag{2}$$

An algebraic behaviour (such as equation (2)) is obeyed at long times if the vacancies themselves perform random walks, so that their probability to return to the origin is of power-law-type [2, 3].

We return now to the original Orwoll-Stockmayer model [12, 13] in which the jumps occur at fixed time intervals, but the jumping bead is chosen randomly; this leads to a simple diffusion of the CM. The same holds for WTD of exponential type, equation (1), when each bead follows its own 'internal clock'. On the other hand, algebraic PD leads to a different behaviour. In figure 2 we show the mean squared displacement of the CM of a chain of $N=5$ beads, when these move according to

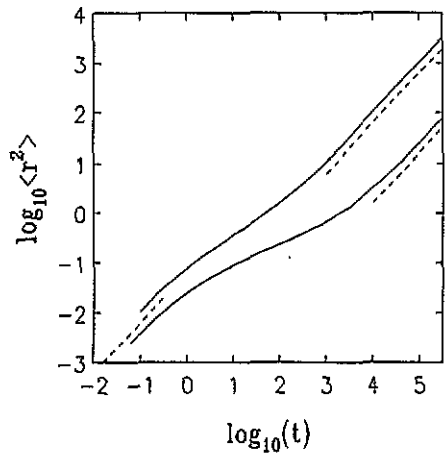

Figure 2. The CM's mean square displacement $\langle r^2(t)\rangle$ for a chain of 5 beads under the PD (2), see text for details. Note the double logarithmic scales. The upper curve is for $\gamma = 1.3$, the lower one for $\gamma = 1.1$. The dashed lines have slope 1.

equation (2) [6]: one observes two different regimes, connected by a crossover region. In the simulations we chose two values for γ (1.3 and 1.1) and let the jumps follow an ordinary renewal process (see below). Note the logarithmic scales and the large time and dynamical ranges required to display the full behaviour, which is quite reminiscent of the polymer-CM motion discussed above.

Now, the appearance under the PD equation (2) of two diffusional regimes is due to the interplay between the memory effects inherent in non-exponential PD and the spatial correlations. Under PD with 'long-time tails' a bead which just performed a jump has a higher probability than the others to perform the next jump. Two consecutive jumps of the same bead, however, cancel each other, and do not lead to any overall motion. The small long-time diffusion coefficients are due to such sequences of repeated jumps, as we proceed to show. In fact, large N are not required for displaying this; focusing on a rigid dumbbell, see figure 1, is sufficient. The dumbbell consists of two beads named H ('Head') and T ('Tail'), connected by a segment of unit length. Each bead jumps according to its own WTD, the waiting-times of the two beads being uncorrelated.

For the WTD two situations can be distinguished:

(i) The WTD for each bead start at $t=0$; this is termed an *ordinary* renewal process (ORP) [15].

(ii) The motion begins long before $t=0$, so that each bead follows an *equilibrium* renewal process (ERP) [15]. For the ERP the interval between $t=0$ and the first jump (the forward recurrence time) obeys the PD

$$\varphi(t)=\int_t^\infty \psi(\tilde{t})\,\mathrm{d}\tilde{t}/\langle t\rangle \tag{3}$$

where we set

$$\langle t\rangle=\int_0^\infty \tilde{t}\,\psi(\tilde{t})\,\mathrm{d}\tilde{t}. \tag{4}$$

The subsequent ERP steps follow the usual (ORP) WTD. Evidently, $\varphi(t)=\psi(t)=\tau^{-1}\exp(-t/\tau)$ for the PD, equation (1) and $\varphi(t)=(\gamma-1)/(1+t)^\gamma$ for equation (2). The difference between (i) and (ii) consists in the waiting-time PD for the first step $\psi_1(t)$, for which $\psi_1(t)=\psi(t)$ for ORP and $\psi_1(t)=\varphi(t)$ for ERP.

In figures 3 and 4 we present in double-logarithmic scales simulation results for the mean squared displacement $\langle r^2\rangle$ of the dumbbell's CM at time t. We also give the average number of jumps n peformed by both beads up to t, $\langle n(t)\rangle$. Figure 3 corresponds to ORP and figure 4 to ERP. For algebraic PD a crossover behaviour ensues, paralleling the results of figure 2. For exponential PD, equation (1), no crossover region is found and a simple diffusive behaviour holds from very early stages on.

Figures 3 and 4 allow us to show the highly correlated situation of the CTRW-motion of the dumbbell. Under exponential PD the situation is hidden, since one has $\langle r^2(t)\rangle\sim t$ and $\langle n(t)\rangle\sim t$. Furthermore for exponential PD one finds for the mean squared displacement in terms of n

$$\langle r^2(n)\rangle\simeq a^2 n \tag{5}$$

where a^2 is the mean squared displacement per step (here $a^2=1$). In the original model [12, 13], starting from a random, Gaussian chain, equation (5) is very well obeyed for

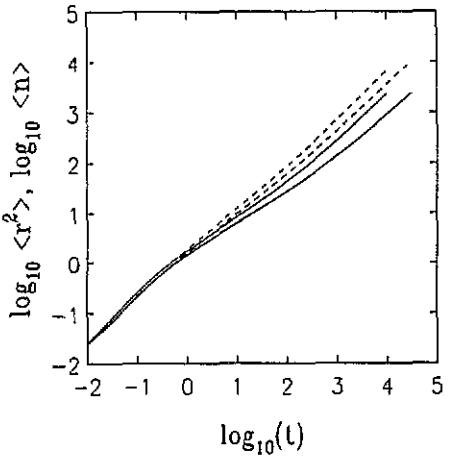

Figure 3. The dumbbell's CM mean square displacement $\langle r^2(t)\rangle$ (full line) and the average number of jumps of the CM, $\langle n(t)\rangle$ (dashed line). Here an ORP is simulated, with equation (2) as PD, $\gamma = 1.3$ (upper) and $\gamma = 1.1$ (lower curves), see text for details.

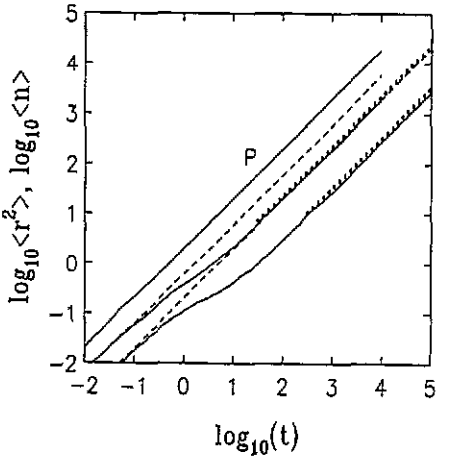

Figure 4. Same as figure 3, but for an ERP. Note that here $n(t) \sim t$ at all times. Included is also a curve for exponential PD, equation (1), (P for Poisson). The dotted lines represent the analytical expression, equation (12).

all n. This one may lead to envisage that, as in a decoupled scheme [4, 7, 8], the following relation holds:

$$\langle r^2(t)\rangle = \sum_{n=0}^{\infty} \langle r^2(n)\rangle \chi_n(t). \tag{6}$$

In (6) the $\chi_n(t)$ is the probability that n jumps (of both H and T) have occurred up to t; the $\chi_n(t)$ can be determined from the pooled [16] (combined) $\psi(t)$ through an inverse Laplace-transform [17]. The meaning of (6) is that the temporal evolution may be directly expressed via the number of jumps.

Equation (6) is, however, not generally valid [8, 18]. Inserting (5) into it one is led to:

$$\langle r^2(t)\rangle \simeq a^2 \sum_{n=0}^{\infty} n\chi_n(t) = a^2\langle n(t)\rangle. \tag{7}$$

The proportionality between $\langle r^2(t)\rangle$ and $\langle n(t)\rangle$ is now clearly at variance with the findings of figures 3 and 4 for broad PD. While at short times $\langle r^2(t)\rangle$ and $\langle n(t)\rangle$ fall together, at longer times their behaviour differs. Hence for broad PD the decoupling of the spatial and temporal aspects, inherent in equation (6) (see [18]), does not hold for $\langle r^2(t)\rangle$.

To understand the findings we now focus on $\langle n\rangle$ and on $\langle r^2\rangle$. Now, $\langle n(t)\rangle = \langle n_H(t)\rangle + \langle n_T(t)\rangle = 2\langle n_H(t)\rangle$, an expression readily evaluated as follows. We notice first that $\chi_n(u)$, the Laplace transform of $\chi_n(t)$, obeys [3]:

$$\chi_n(u) = \psi_1(u)[\psi(u)]^{n-1}[1-\psi(u)]/u \tag{8}$$

so that holds:

$$\langle n(u)\rangle = 2\langle n_H(u)\rangle = 2\psi_1(u)/\{u[1-\psi(u)]\} \tag{9}$$

with $\psi_1(u)=\psi(u)$ for ORP and $\psi_1(u)=[1-\psi(u)]/(u\langle t\rangle)$ for ERP. Equation (9) gets to be particularly simple for ERP, $\langle n(u)\rangle = (2/\langle t\rangle)u^{-2}$, i.e.

$$\langle n(t)\rangle = 2t/\langle t\rangle \tag{10}$$

as is evident from figure 4. The dependence on the WTD enters then only through $\langle t\rangle = \tau$ for (1) and $\langle t\rangle = 1/(\gamma-1)$ for (2). For ORP equation (10) is also obeyed for t large; whereas for small t one finds from equation (8) $\langle n(t)\rangle = 2\gamma t$. We note that the result, equation (10), is connected to the renewal theorem ([15] p 46 ff) and holds for $\langle t\rangle < \infty$. The short-time behaviour is due to $\psi_1(0)\neq 0$; for $\psi_1(0)=0$ the dependence of $\langle n(t)\rangle$ on t is no longer linear.

We now turn to the mean squared displacement and display in figure 5 $\langle r^2(n)\rangle$. In particular for ERP with broad PD the curves show clear fluctuations between even and odd n, superimposed on a nearly linear increase. The fluctuations arise because the displacements due to two subsequent jumps of the same bead cancel. This feature suggests to decouple the CTRW-process at the two-jump level; as we proceed to show, this approximation (which neglects higher-order correlations) works very well.

We view then two subsequent jumps of the CM as one, renormalized, step. The CM moves by ± 2 if the jumps involve both beads (probability q) and by 0 otherwise (probability $p=1-q$). The mean squared displacement per renormalized step is now $4q=4(1-p)$. To calculate p we assume (to fix the ideas) H to make the first jump of the renormalized step. Let us denote by t_1 the time it takes to perform the next jump of H, and by t_2 the corresponding time for T. Note that t_1 follows from ORP WTD, while t_2 obeys the ERP WTD (the last assumption is certainly correct in the long-time regime). Now p is the probability that $t_1 < t_2$ and is given by:

$$p = \int_0^\infty \mathrm{d}t_2 \varphi(t_2) \int_0^{t_2} \mathrm{d}t_1 \psi(t_1). \tag{11}$$

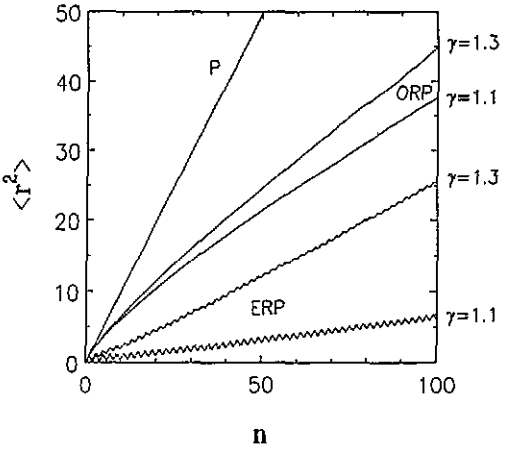

Figure 5. The CM's mean square displacement $\langle r^2\rangle$ as a function of the number of jumps n. The curve (P, Poisson) follows for an exponential PD, equation (1) whereas the curves for ERP and ORP are based on equation (2) in which $\gamma = 1.3$ and $\gamma = 1.1$ were set.

From equation (11) one finds for the exponential PD $p=\frac{1}{2}$ (as expected), whereas for the power-law PD, equation (2) $p=\gamma/(2\gamma-1)$ follows. We now assume that different renormalized steps are uncorrelated. The exponential PD leads again to $\langle r^2(t)\rangle = 2t/\tau$, whereas for algebraic PD, equation (2) one obtains for p as above and t large

$$\langle r^2(t)\rangle = \frac{4(\gamma-1)^2}{2\gamma-1}\,t. \tag{12}$$

The corresponding short- and long-time behaviours are also given in figures 3 and 4. The crossover from the short-time behaviour ($\langle r^2(t)\rangle = 2\gamma t$ for ORP and $\langle r^2(t)\rangle = 2(\gamma-1)t$ for ERP) to the long-term form, equation (12) takes place at times corresponding to a few first jumps of the dumbbell.

Summarizing, we have analysed the CTRW motion of a rigid dumbbell, this being the simplest model of random walkers connected via holonomic constraints. For broad PD the motion resembles that of macromolecules in melts, displaying two diffusive regimes, with a broad crossover region in between. The reason for this is a coupling between the temporal and geometrical aspects of the CTRW-process. Here we obtained approximate expressions for the diffusion coefficients in the two regimes. Interestingly, the features due to the temporal-spatial coupling are obscured when only exponential PDs are used, so that employing algebraic PD is very helpful.

Acknowledgment

We acknowledge thankfully support by the DFG (SFB 60), by the Fonds der Chemischen Industrie and by the NATO research grant RG 0115/89.

References

[1] Scher H and Montroll E W 1975 *Phys. Rev.* B 12 2455
[2] Bendler J T and Shlesinger M F 1985 *The Wonderful World of Stochastics* ed M F Shlesinger and G Weiss (Amsterdam: North-Holland) p 31
[3] Blumen A, Klafter J and Zumofen G 1986 *Optical Spectroscopy of Glasses* ed I Zschokke (Dordrecht: Reidel) p 199
[4] Blumen A, Klafter J and Zumofen G 1986 *Fractals in Physics* ed L Pietronero and E Tossatti (Amsterdam: North-Holland) p 399
[5] Eisenberg E, Havlin S and Weiss G H 1994 *Phys. Rev. Lett.* 72 2827
[6] Schieber J D, Biller P and Petruccione F 1991 *J. Chem. Phys.* 94 1592
[7] Blumen A, Klafter J, White B S and Zumofen G 1984 *Phys. Rev. Lett.* 53 1301
[8] Klafter J, Blumen A and Shlesinger M F 1987 *Phys. Rev.* A 35 3081
[9] Doi M and Edwards S F 1986 *The Theory of Polymer Dynamics* (Oxford: Oxford University Press) ch 6
[10] de Gennes P-G 1971 *J. Chem. Phys.* 55 572
[11] Lodge T P, Rotstein N A and Prager S 1990 *Adv. Chem. Phys.* 79 1
[12] Orwoll R A and Stockmayer W H 1969 *Adv. Chem. Phys.* 15 305
[13] Verdier P H 1970 *J. Chem. Phys.* 52 5512
[14] Glarum S 1960 *J. Chem. Phys.* 33 639
[15] Cox D R 1967 *Renewal Theory* (London: Methuen)
[16] Cox D R and Smith W L 1954 *Biometrica* 41 91
[17] Schiessel H, Alemany P and Blumen A 1994 *Progr. Colloid. Polym. Sci.* in press
[18] Klafter J, Blumen A, Shlesinger M F and Zumofen G 1990 *Phys. Rev.* A 41 1158